Optical fiber pressure sensor using extrinsic Fabry–Perot interferometry (EFPI); a theoretical study

HARRY RAMZA[a*], NORHANA ARSAD[b], FAIZAR ABDURRAHMAN[b], LATIFAH. S. SUPIAN[a]
MOHAMMAD SYUHAIMI AB-RAHMAN[a]
[a]Spectrum Technology Research Group, Department of Electrical, Electronic and Systems Engineering, Faculty of Engineering and Built Environment, Universiti Kebangsaan Malaysia, 43600 UKM-Bangi Campus, Selangor, Malaysia
[b]Laboratory of Photonics, Institute of Microengineering and Nanoelectronics, Universiti Kebangsaan Malaysia, 43600 UKM-Bangi Campus, Selangor, Malaysia

This paper discuss the theoretical analysis and experimental results of pressure measurement using optical fiber sensor with cladding modification and coating with ZnO (Zinc Oxide as sensitive material to enhanced the performance of sensor that's uses as sensing probe inside the pressure chamber. The modification fiber was coated by dip coating deposition method. During measurement of fiber sensor, the refractive index changes based on different pressure given. The changing of refractive index affects the phase different of optical path along optical fiber. Extrinsic Fabry – Perot Interferometer (EFPI) method is used to obtain the data measurement. Pressure variables prearranged from 0 to 104.8 mBar. The experiment outputs are intensity of reflection light and variety of pressure. The sensitivity of sensor obtained is 1.1% with swelling thickness from 0 to 1.181 μm.

1. Introduction

POF (Plastic Optical Fiber) can be used as a pressure sensor. The operational principle of this sensor is calculating the light intensity and the aspects of sensor work is determined by an output examination of a low efficiency EFPI (Extrinsic Fabry –Perot Interferometer) to generate phase different sensitivity [1-3]. The pressure sensitivity and frequency response of the sensor will increase when an interaction of sensing layer occurs between material layer with air pressure [2-8]. Figure 1 shows an element of the detector of the ZnO (Zinc Oxide) layer with refractive index (n_x) and thickness (dL) in the linkage of two different media: medium-1 on the middle of the core refractive index (n_1) and the medium-2 on the outside of the refraction index (n_2). Fresnel reflection coefficient arises from the non-matching refractive index at the boundary of detector layer $(R_1$ and $R_2)$ that is considered low enough to be able to contribute many ways in order to ignore or avoid the reflected light of interferometer. Therefore, reflected light detection at the probe tip can be used to measure the air pressure [9].

The probe condition that is coated by ZnO material shown at Fig. 2. Fig. 2 (a) shows ZnO layer along the probe tip, as look figure 2 (b) of probe tip.
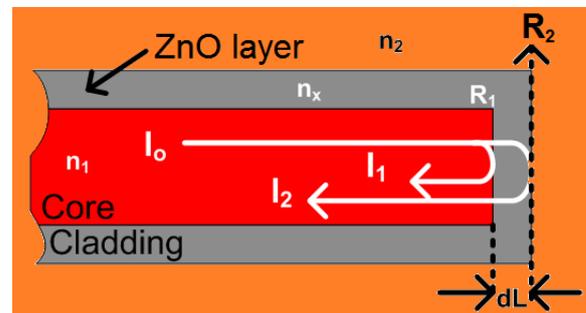
Fig. 1. Principal operation of low-finesse Fabry-Perot interferometer pressure detector

The probe tip shows the uneven cutting of the optical fiber with probe diameter at this Fig.-2 (b) around 0.6 mm. ZnO layer condition characteristic can be seen at Fig. 2 (c) and (d) with zooming factor of SEM image are 1000 times and 5000 times respectively. This modification layer has layer-density around ±1 μm of the coating slit pattern homogeneity. To readout of measurement line scale from Fig. 2 (a), (b), (c) and (d) uses amount 1 mm, 100 μm, 18 μm and 5 μm scale respectively.
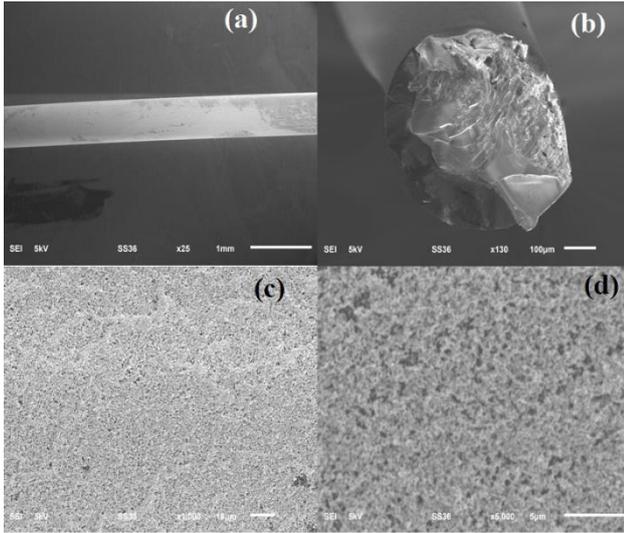
Fig 2. SEM images of ZnO layer on the plastic optical fiber, (a). ZnO coated along the POF (b). The tip part of POF probe, (c) and (d). SEM image of ZnO layer condition.

This paper discusses measurements of the low–finesse Fabry–Perot interferometer pressure sensor. The pressure measurement setup of the device and the performance of the sensor are analyzed. In the following subsections, describes a case in which the interferometer is illuminated with normal light test is followed by consideration of the lighting effects of interferometer with a divergence output of optical fiber.

2. Illumination of Sensing Layer at Normal Incident Light

The overlapping of light occurs due to the superposition of the light intensity of the reflection I_1 and I_2 from two boundaries. It is a result of the separation of incoming light in normal conditions (Fig. 1)[10].

$$I_0 = I_1 + I_2 + 2\sqrt{I_1 I_2} \cos \Phi \qquad (1)$$

Where ϕ is the total of phase difference caused by the difference of the optical path length of the two reflected light components. When light is influenced by pressure at the probe tip zone, ϕ can be said to be composed of two components; ϕ and $d\phi$, which are phase bias that indicates the working point from the different time of the signal and the emerged light due to the changes of pressure at the ZnO layer of the probe respectively[10].

$$\Phi = \phi + d\phi \qquad (2)$$

By inserting equation (2) into the equation (1), we obtained a complete equation as[10],

$$I_0 = I_1 + I_2 + 2\sqrt{I_1 I_2} \left(\cos \phi \cos d\phi - \sin \phi \sin d\phi\right) \quad (3)$$

For optimum sensitivity and linearity it is expected that we assign ϕ- phase bias at the quadrature point, where $\phi = (2m + 1)\pi/2$, (m is an integer value) by tuning the wavelength of the laser source. At first quadrature point, $\phi = \pi/2$, and for the smallest value $d\phi$, equation (3) can be shortened as[10],

$$I_0 = I_1 + I_2 - 2\sqrt{I_1 I_2} \sin(d\phi) \qquad (4)$$

In this situation, the output of interferometer that is detected by a photodiode consists of a pressure effect, the change of time, the intensity modulation dI_0 where it is linearly dependent on a $d\phi$ component and an I_{dc} component[10],

$$dI_0 = -2\sqrt{I_1 I_2} \, d\phi \qquad (5)$$

$$I_{dc} = I_1 + I_2 \qquad (6)$$

I_1 and I_2 can be written in the incident intensity I and the Fresnel reflection coefficient and r_1 and r_2 are defined by the refractive index mismatch at the boundary layer of the detector[9-11]

$$I_1 = I \cdot R_1, \ I_1 = I \cdot (1 - R_1)^2 \cdot R_2 \qquad (7)$$

where,

$$R_1 = \frac{n_1 - n_x}{n_1 + n_x}, \text{and } R_2 = \frac{n_x - n_2}{n_x + n_2} \qquad (8)$$

From equation (5) and (7) the phase sensitivity of the interferometer is defined as the intensity modulation of the phase-shifting unit interferometer $dI_0/d\phi$, and the DC level of I_{dc} can be written as an equation[10],

$$\frac{dI_0}{d\phi} = -2I(1 - R_1)\sqrt{R_1 R_2} \qquad (9)$$

$$I_{dc} = I|R_1 + (1 - R_1)^2 \cdot R_2| \qquad (10)$$

These equations are used to maximize the phase-sensitivity selection I, R_1 and R_2, but it is important to note that these parameters also affect the DC component. The DC component is the unwanted portion of the output of the interferometer, as it generates huge photo currents in the presence of noise absorbers that can dominate the noise characteristics of the diode. In addition, if the current DC level is too high, it will saturate the photodiode, limiting the maximum phase sensitivity that can be achieved with the rise-current of I.

3. Fringe Visibility

The difference in power coefficients of optically reflected light from the end of the optical fiber with or without cladding modification is mostly small, around 4% in Fresnel reflection result. The many reflected lights in low-finesse EFPI can for this reason consequently be

ignored in the calculation[12]. Equation (4) can be substituted into the other symbol I_x, this simbol is a summation of the Fresnel reflection. In the end, the simplified equation will be[3],

$$I_0 = I_x \left(1 + \frac{2\sqrt{I_1 I_2}}{I_x} \sin(d\phi) \right)$$

where,

$$I_x = I_1 + I_2 \tag{11a}$$
$$I_o = I_x(1 + V \sin(d\phi)) \tag{11b}$$

$$\frac{I_0}{I_x} - 1 = V \sin(d\phi) \tag{11c}$$

thus,

$$V = \frac{I_0 - I_x}{I_x \sin(d\phi)} \tag{12}$$

Equation (12) describes the visibility (V) of the light measured based on the phase difference ($d\phi$), source intensity (I_0) and Fresnel reflection intensity (I_x). Phase difference is influenced by several factors such as opto-pressure constant (ε), length of the sensing probe (l), thickness layer (dl), wavelength (λ) and refractive index of material (n). If the phase difference is equal to zero, then the result is infinite. In the case of the phase difference is equal to one, then the visibility is minimal or the intensity is low. The Fresnel reflection light is weak and the pressure measurement is equal to low-pressure.

4. Sensitivity Calculation Base on Pressures Variety

Based on equation (4), in general phase change due to air pressure and vapours can be written as,

$$d\phi = 2\beta.l = 2nk.l \tag{13}$$

for changes due to pressure;

$$\frac{d\phi}{dp} = 2 \frac{\partial(\beta l)}{\partial p}$$

$$\frac{d\phi}{dp} = 2 \left(\frac{\partial\phi}{\partial\beta} \frac{\partial\beta}{\partial p} \right) + 2 \left(\frac{\partial\phi}{\partial l} \frac{\partial l}{\partial p} \right)$$

$$\frac{d\phi(p)}{dp} = \left(\frac{\partial\phi}{\partial\beta} \cdot \frac{\partial\beta}{\partial p} + \frac{\partial\phi}{\partial\Delta l} \cdot \frac{\partial\Delta l}{\partial p} \right)$$

$$\frac{d\phi(p)}{dp} = 2l \frac{\partial\beta}{\partial p} + 2\beta \frac{\partial l}{\partial p} = 2kl \frac{\partial n}{\partial p} + 2nk \frac{\partial l}{\partial p} \tag{14}$$

$$\frac{d\phi(p)}{dp} = \frac{4\pi l}{\lambda} \frac{\partial n}{\partial p} + \frac{4\pi n}{\lambda} \frac{\partial l}{\partial p}$$

$$\frac{d\phi(p)}{dp} = \frac{4\pi}{\lambda} \left(l \frac{\partial n}{\partial p} + n \frac{\partial l}{\partial p} \right)$$

$$\frac{d\phi(p)}{dp} = \frac{4\pi}{\lambda} \left(l\varepsilon + n \frac{\partial l}{\partial p} \right)$$

In the equation above, the first term can be represented as opto-pressure constant (ε), that is shown below;

$$\varepsilon = \frac{1}{n_j} \frac{\partial n_j}{\partial p} = 2.68 \times 10^{-7} mBar^{-1} \tag{15}$$

where the symbol $j = 1, 2$; represent the core and cladding refractive indices. The value shown above is the value of refractive index change in each 1 mBar pressure. Equation (16) shows the change of the length of the fiber detector due to vacuum chamber pressure[13].

$$\frac{\partial\phi(p)}{\partial p} = \frac{4\pi}{\lambda} \left(l\varepsilon + n \left(\frac{A \cdot r_0^2}{E(r_0^2 + r_1^2)} (1 - 2\mu)P \right) \right) \tag{16}$$

Equation (16) states that the phase changes due to air pressure. These changes are caused by the reaction of detector refractive index to the air pressure or also known as opto-pressure coefficient. This coefficient is attuned by real measurement given or adjusted using test pressure division value. The equation can also resemble the sensitivity pressure detector value, $\zeta = \partial\phi(p)/\partial p$.

5. Configuration of Optical Fiber EFPI

The basic configuration of an EFPI pressure sensor is demonstrated in Fig 3. The system consists of a white light source, a spectrometer, fiber-optics and a detector head. The sensor head has been modified using ZnO layer (see Fig 1).

The white light is injected from terminal A (white light source) and will go through terminal C (coupler) and be reflected back due to the ZnO probe. The residual light will pass through terminal B (spectrometer). The phase difference between the refractive index of ZnO layer will change the light intensity. Equation (4) states that ϕ the phase shift equation can be expressed as[13-15];

$$d\phi = 2 \cdot \beta \cdot dl = 2 \cdot n \cdot k \cdot dl = 4\pi \frac{n \cdot dl}{\lambda} \tag{17}$$

where l is the area of detection layer at the edge of optical fiber, n is refractive index of ZnO and k is a wave number or a scalar quantity that only depends on the wavelength, λ.
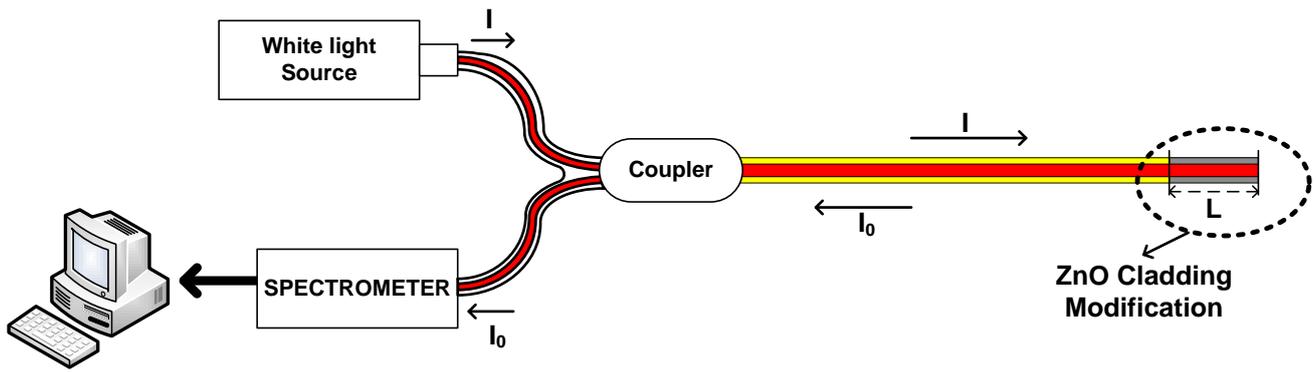
Fig. 3. Configuration of EFPI pressure sensor.

In equation (17), phase change occurs because of the thickness of the layer detector (dl) at the end of the optical fiber. The expression dl in the equation is a phase difference factor that can be written as[13],

$$dl = \frac{A \cdot r_0{}^2}{E(r_0{}^2 + r_1{}^2)}(1 - 2\mu)P \qquad (18)$$

where A is area of layer detection, $r_0{}^2$ and $r_1{}^2$ are radii of layer detection, and E is Young Modulus of optical fiber. Plastic optical fiber follows the specification which is given in Table 1 below,

Table 1. Specification of the ESKA® Plastic Optical Fiber

	Core	Cladding
Material	PMMA resin	Fluorinated polymer
Diameter (typical)	980 µm	1000 µm
Young's modulus	3.09 GPa	0.68 GPa
Poisson's ratio	0.3	0.3
Refractive index	1.492	1.405
Yield strength	82 MPa	
Transmission loss (@ 650 nm)	200 dB km^{-1}	
Maximum operating temperature	70 "C	
Approximate weight	1 g m^{-1}	

Table 1 shows specification of plastic optical fiber and fiber sensor measured different level of pressure in the vacuum chamber. The detector is placed in the middle of the chamber and covered by the iron rod. The rod also functioned to protect of the head sensor.
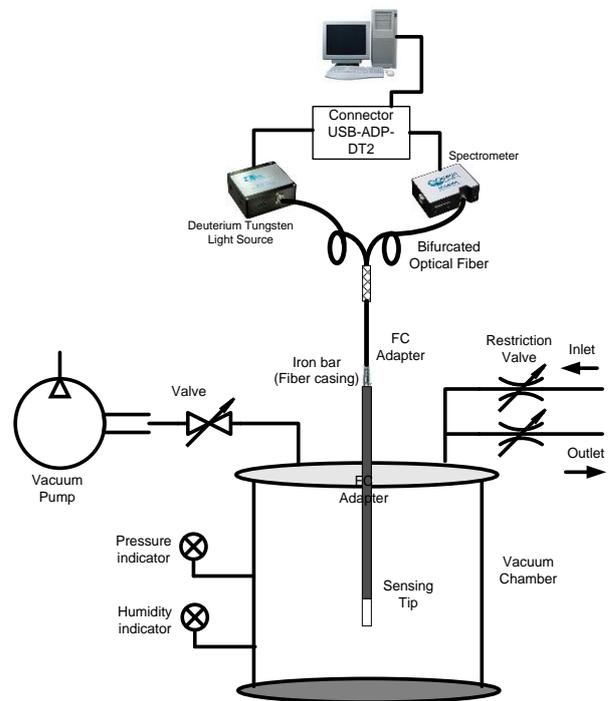
Fig. 4. Experimental setup of pressure sensor[16].

In line with Fig 4, deuterium tungsten halogen light is sent to the trunk fiber optic by using a branched Fabry-Perot interferometer setup. Light received from the detector head will first be processed through an Ocean Optics USB4000 spectrometer. The results from spectrometer will process further by computer. 2 x 1 optical coupler is applied in the experiment and equipped with SMA connector and 1-branch is free[16]. At about 3 cm from the free end of this fiber, The cladding sensor is removed by chemical etching using a solution of acetone and fine grade sandpaper. Measurement is done by providing a change of pressure in the chamber using the vacuum pump. The exerted regular pressure can be seen from the valve position indicator through the pressure and humidity indicators.

6. Result and discussion

The data collection was done as the pressure in the vacuum chamber is varied on regular basis using a mechanical valve. Air pressure is reduced by drawing air through the oil-less piston vacuum pump. The air duct of the chamber test is divided into two parts, namely the vacuum pump and pressure gauge (HHP-90). Air pressure detection device is placed on top of a chamber test, so it will be easier to connect the USB4000 spectrometer.

The light source was a white light (Tungsten Halogen Ocean Optics USB-DT). This light source produces light in the ultraviolet, visible and infrared spectrum. Fig 5 represents the results of light intensity detected by going through each wavelength of the spectrum and the light intensity unit is counts.
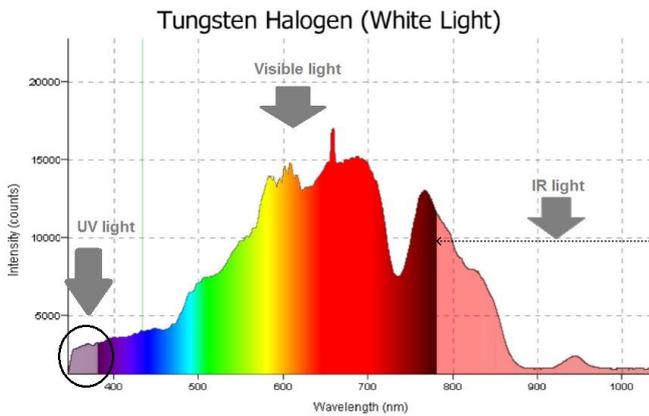
Fig. 5. The wavelength spectrum of white light.

Fig 6 illustrates the measured signal from the fiber optic Fabry-Perot interferometer with low coherence light source. In this figure, the intensity of incoming light, the reflected light and the transmission light are represented with the black line, blue dotted line and red-circle dotted line respectively, and the light intensity unit is arbitrary unit.
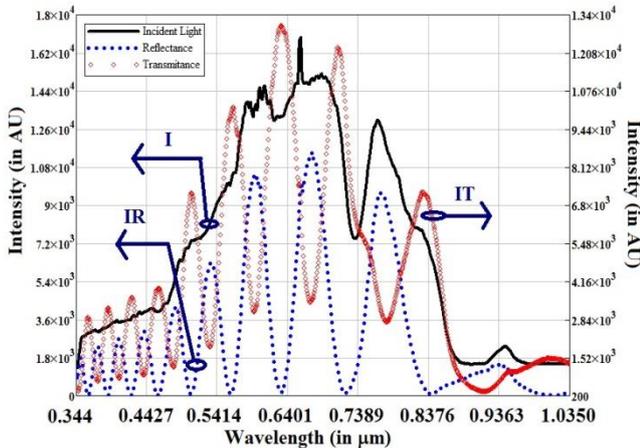
Fig. 6. Intensity measurement from optical fiber using FPI at 104.80 mBar pressure vacuum chamber.

Fig 6 shows that as the bigger of the wavelength grow bigger, the absorbance patterns will be increasingly tenuous (for one period of the wave). Fig 7 explains that different wavelengths will give different absorption values and the percentage of light emitted through the sensor head. It will change as the wavelengths vary; 345 nm up to 1040 nm. The pressure exerted in the light intensity measurement is 104.80 mBar.
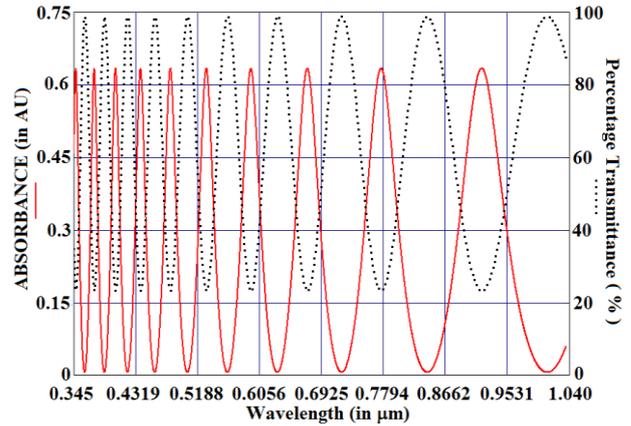
Fig. 7. The light absorption and the percentage of the light transmission compared to the used wavelength.

Fig 8 shows the variation of pressure due to vacuum pump effect that is used in this experiment. It will produce a thicker coating or swelling. The result is calculated based on equation (18) which gives Young modulus of optical fiber and Poisson ratio. The slope of the line equation obtained is 0.011, which represents the change in the pressure needed to test the thickness of the modified coating, generally referred to as the sensitivity of the sensor device. The sensitivity is very small due to the influence of changes in the refractive index of the cladding, where the propagation of light is very slow due to the wide applied pressure difference.
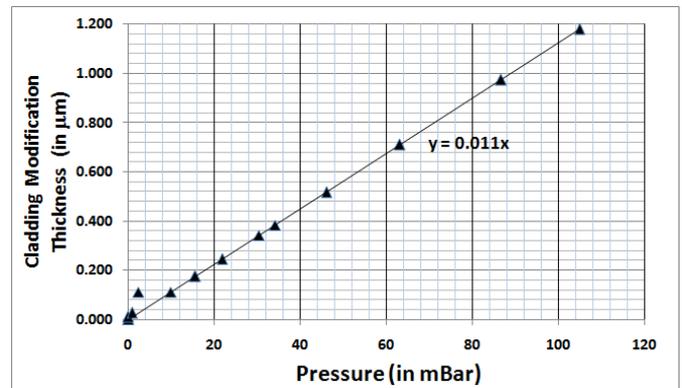
Fig. 8. Pressure changes compared to the swelling thickness of head sensor.

Fig 9 (a), (b), (c) give the phase difference value at several wavelengths. The phase difference values are calculated from 355 nm until 1055 nm. Phase difference of θ: 0^0 to 1^0 (degree) are influenced by the pressure of the

chamber test 0 – 2.48 mBar. Phase difference from 2 to 12 degrees are affected by the pressure chamber being at 9.91mBar - 34.1 mBar and the phase difference from 12^0 to 82^0 degrees are influenced by pressure from 34.1 mBar until 104.8 mBar.
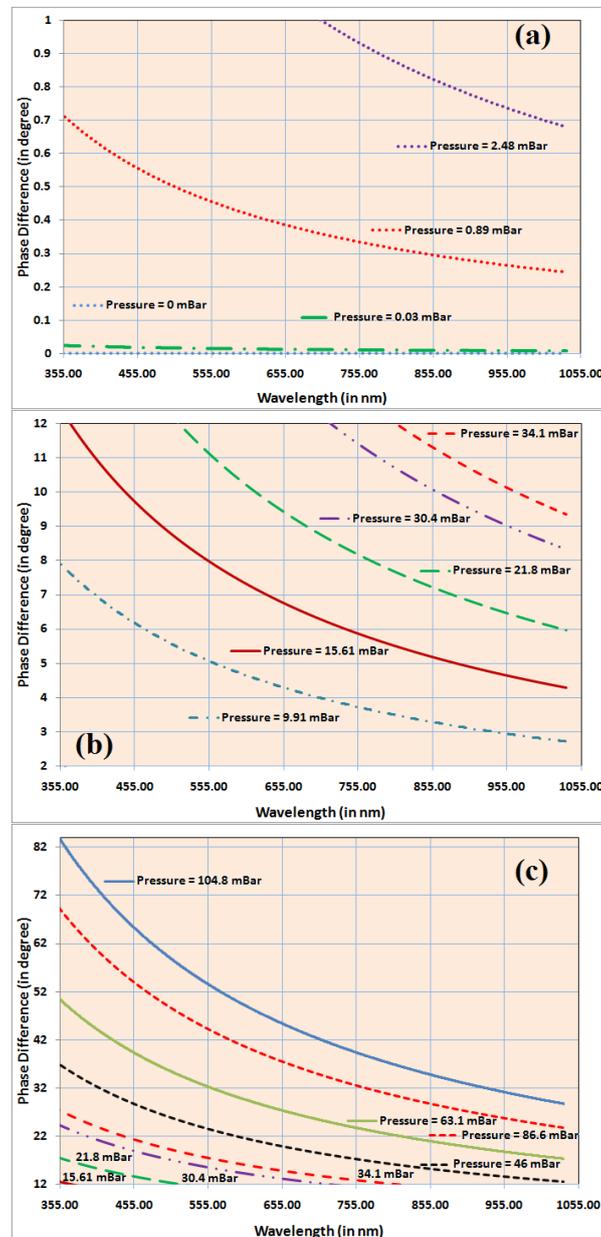
Fig. 9. The phase changes of head sensor caused pressure effect on each wavelength.
The pressure changes (a) P <2.48 mBar; (b) 9.91 mBar < P<34.1 mBar; (c) P ≥34.1 mBar.

The distinction of graph a, b and c are the initial values due to changes in the pressure chamber. Higher pressure affected a phase change and it is more pronounced at each wavelength. The phase change will affect an intensity change which is accepted by the spectrometer, as shown in Fig. 5. Light intensity achievement is the initial reflected light from the head of the optical fiber receiver end portion.

7. Conclusion

In this experiment the initial swelling process size is 0.000338 um and the vacuum pressure is 0 mBar. The vacuum pressure for swelling size of 1.181000 μm is 104.8 mBar, even though sensor sensitivity is very small (0.011) due to thin coating process. However the sensor sensitivity can be improved using thicker coating by repeatedly using immersing process. In the future, the improvement of the methodology and coating process will be revised to get a better result.

References

[1] S. H. Aref, H. Latifi, M. I. Zibaii, M. Afshari, Opt. Com. **269,** 322 (2007).

[2] J. Joung, K. C. Kim, J. Korean. Phys. Soc. **51,** 249 (2007).

[3] J. M. López-Higuera, Optical sensors: fundamentals, current situation and future trends, in Optical Sensors, Ed. J. M. López-Higuera, Universidad de Cantabria, Santander, Spain (1998).

[4] A. Maddu, H. Zain, S. Sardy, J. Optoelectron. Adv. Mater. **9,** 2362 (2007).

[5] M. Jędrzejewska-Szczerska, B. B. Kosmowski, R. Hypszer, Phot. Let of Poland. **1,** 61 (2009).

[6] C. E. Lee, H. F. Taylor, Sensors for smart structures based on the fabry-perot interferometer, in Fiber optic smart structures, Ed. E. Udd, Wiley Interscience, Michigan (1995).

[7] T. Zhu, D. Wu, M. Liu, D. W. Duan, Sensors. **12,** 10430 (2012).

[8] M. F. Miller, M. G. Allen, E. Arkilic, K. S. Breuer, M. A. Schmidt, Proc. International Conference on Solid State Sensors and Actuators. Chicago, IL, Ed. IEEE, 1997, p. 1469

[9] Z. Ran, Y. Rao, J. Zhang, Z. Liu, B. Xu, J. Light. Tech. **27,** 5426 (2009).

[10] P. C. Beard and T. N. Mills, Appl. Opt. **35,** 663 (1996).

[11] G. Z. Xiao, A. Adnet, Z. Zhang, F. G. Sun, C. P. Grover, Sens and Act A: Phys. **118,** 177 (2005).

[12] J. S. Zeakes, K. A. Murphy, A. Elshabini-Riad, R. O. Claus, Proc. Lasers and Electro-Optics Society Annual Meeting. Boston, MA, Ed. IEEE, Piscataway, NJ, 1994, p. 235

[13] Q. Yu, X. Zhou, Photon. Sens. **1,** 72 (2011).

[14] A. Kumar, R. Jindal, R. K. Varshney, S. K. Sharma, Opt. Fiber. Tech. **6,** 83 (2000).

[15] F. Perennes, P. C. Beard, T. N. Mills, Appl Opt. **38,** 7026 (1999).

[16] H. Ramza, F. Nasimi, K. A. Ishak, N. Arsad, M. S. Ab-Rahman, Proc. Int Conf on Eng and Built Env. Selangor, MY, Ed. Universiti Kebangsaan Malaysia, 2012, p. 46.

_____
[*]Corresponding author: hramza@eng.ukm.my